PIER M

A Stable and Efficient Interpolation Method for Two-Dimensional Periodic Green's Functions

Lian Feng Ma[1, 2], Qing Guang Zhao[3], Chong Guo[4], and Yi Ren[4, *]

[1]*School of Electronic Science and Engineering, University of Electronic Science and Technology of China, China*
[2]*Chengdu Aircraft Design and Research Institute, Aviation Industry Corporation of China, China*
[3]*Shanghai Institute of Satellite Egineering, China*
[4]*School of Electronic Engineering, Xidian University, China*

ABSTRACT: This paper presents an efficient and stable interpolation method for calculating two-dimensional periodic Green's function and its gradient. The method consists of two steps: constructing an interpolation table in the first step and using linear interpolation to extract the desired Green's function from the interpolation table in the second step. In the construction of the interpolation table, several properties of the two-dimensional periodic Green's function are fully utilized, which minimize the size of the interpolation table. When the elements in the interpolation table are computed, all possible singular terms are removed, ensuring that the interpolation function maintains high linearity even under extreme skew periodic grids. This means that linear interpolation can guarantee sufficient accuracy. Numerical results demonstrate effectiveness of the proposed method, making it suitable for combining with numerical methods for electromagnetic field calculation and analysis of periodic structures.

1. INTRODUCTION

In electromagnetic field analysis, Green's function is the core of many computational methods. In complex scenarios, whether for analytical or numerical calculations, the efficient estimation of Green's functions often becomes a bottleneck that limits the effectiveness of these computational methods. Two-dimensional periodic Green's function is the core for the analysis of two-dimensional periodic structures. As we know, two-dimensional periodic structures have a wide range of applications, such as frequency-selective surfaces [1], phased array antennas [2], and metasurfaces [3]. When the entire unit of a two-dimensional periodic structure is analyzed, multiple calculations of periodic Green's function are often required, so the fast estimation of the two-dimensional periodic Green's function within the entire periodic unit is particularly important.

The original form of two-dimensional periodic Green's function is based on an infinite series of free-space Green's functions, which converges very slowly. To improve convergence speed, acceleration methods [4] such as the Ewald's method [5], Shank's transform [6], and Kummer's decompositions [7] have been proposed. However, even with these acceleration methods, the computational efficiency is still very low when field calculations are performed within the entire periodic unit, such as the calculation of matrix elements in method of moment (MoM), which cannot meet the requirements of practical calculations. Due to this reason, interpolation methods have emerged.

Generally, in interpolation methods, the first step is to pre-construct an interpolation table within the periodic unit. Then, based on the relationship between the source point and obser-

vation point, the Green's function at the observation point is obtained through interpolation from the interpolation table. In existing publications on two-dimensional periodic MoM, interpolation methods are inevitably used [8–10]. However, these publications [8–10] do not provide details on the construction of interpolating table and interpolation schemes. Moreover, the interpolation tables used in these publications are constructed within the entire periodic unit and do not fully utilize the properties of the periodic Green's function. In this paper, we will demonstrate that it is not necessary to construct the interpolation table within the entire unit. In fact, by using suitable transformations and interpolations, constructing the interpolation table within a quarter of the unit is sufficient to be used to obtain the Green's function values at any position of the entire unit.

This paper is organized as follows. Section 2 introduces the calculation of the periodic Green's function based on the Ewald method. Section 3 presents the construction of the interpolation table and interpolation scheme. Section 4 provides two numerical examples to illustrate the effectiveness of the proposed method. In, Section 5, conclusions are provided.

2. PERIODIC GREEN'S FUNCTION

In this section, we introduce the expressions for the periodic Green's function and its gradient.

Let us consider the periodic structure shown in Figure 1. In the figure, U represents the space under study, which completely encloses the periodic structure unit. S_U is the transverse area of U. Within U, **R** represents the vector from the real source point to the observation point, **r** (x, y, z) the position of the observation point, and **r'** (x', y', z') the position of the real source point. $\mathbf{a}_1$ and $\mathbf{a}_2$ are the unit direction vectors in

$$U := \{(ua_1\cos\phi, (va_2 + ua_1\sin\phi), z) \in R^3 \mid u, v \in [0, 1], z \in R\}$$

$$\mathbf{R} = \mathbf{r} - \mathbf{r}' \quad R = |\mathbf{R}|, \quad \mathbf{r}, \mathbf{r}' \in U$$

$$\mathbf{R}_{nm} = \mathbf{r} - \mathbf{r}' - \boldsymbol{\rho}_{nm} \quad R_{nm} = |\mathbf{R}_{nm}|$$

$$S_U = a_1 a_2 \cos\phi$$

$$(a_1 = |\mathbf{a}_1|, \quad a_2 = |\mathbf{a}_2|)$$

$$\boldsymbol{\rho}_{nm} = n\,\mathbf{a}_1 + m\,\mathbf{a}_2$$

$$= \hat{\mathbf{x}}na_1\cos\phi + \hat{\mathbf{y}}(ma_2 + na_1\sin\phi)$$
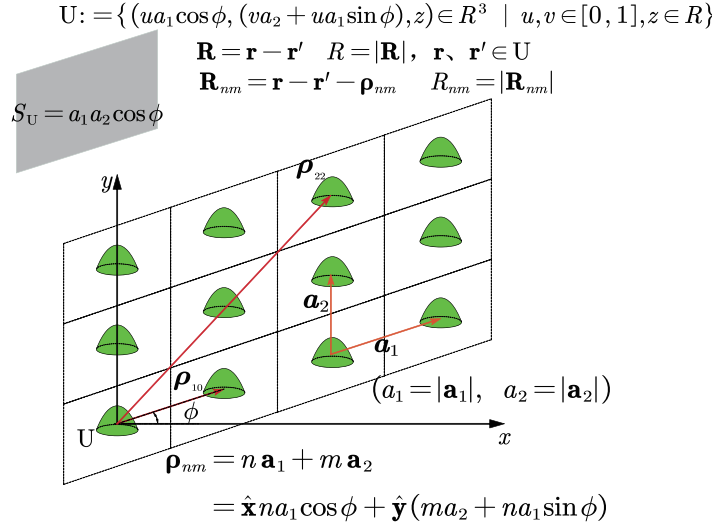
FIGURE 1. 3D objects arranged in 2D periodic lattices.

the two periodic directions. $\boldsymbol{\rho}_{nm}$ is the position vector of the (n, m)th periodic unit relative to U, and $\mathbf{R}_{nm}$ is the position vector from the virtual source point inside the (n, m)th periodic unit to the observation point inside U. It should be noted that U is the $(0, 0)$th unit, with its transverse section parallel to the *xoy* plane and its longitudinal direction parallel to the z-axis.

Based on the Floquet theorem, the expression for the periodic Green's function G_p in terms of a series of the image Green's function can be written as follows [8].

$$G_p(\mathbf{r}, \mathbf{r}') = G_p(R) = \frac{1}{4\pi}\sum_{n,m}\frac{e^{-jkR_{nm}}}{R_{nm}}e^{-j\boldsymbol{\beta}_0\cdot\boldsymbol{\rho}_{nm}} \quad (1)$$

Notice that k is the wave number of interested region while $\boldsymbol{\beta}_0$ denotes the phase constant vector in free space.

The convergence of above series is very slow. The Ewald method is the most widely used method to accelerate the convergence of (1), thus in this paper we adopt the Ewald method to expand G_p. By separating G_p into the spatial-domain part G_{spat} and the spectral-domain part G_{spec}, the new expression in series is as follows [8].

$$G_p(R) = G_{spat}(R) + G_{spec}(R) \quad (2)$$

$$G_{spat}(R) = \frac{1}{8\pi}\sum_{n,m}\frac{e^{-j\boldsymbol{\beta}_0\cdot\boldsymbol{\rho}_{nm}}}{R_{nm}}\sum_{\pm}e^{\pm jkR_{nm}}$$

$$\cdot\mathrm{erfc}\left(R_{nm}E \pm \frac{jk}{2E}\right) \quad (3)$$

$$G_{spec}(R) = \frac{1}{4S_U}\sum_{n,m}\frac{e^{-j\mathbf{k}_t(n,m)\cdot\mathbf{R}}}{jk_z(n,m)}$$

$$\cdot\sum_{\pm}e^{\pm jZk_z(n,m)}\mathrm{erfc}\left(\frac{jk_z(n,m)}{2E} \pm ZE\right) \quad (4)$$

In above equations

$$\mathrm{erfc}(z) = 1 - \frac{2}{\sqrt{\pi}}\int_0^z e^{-\xi^2}d\xi \quad (5)$$

$$X = x - x', \quad Y = y - y', \quad Z = z - z' \quad (6)$$

$$\gamma = \alpha + j\beta = jk \quad (7)$$

$$\mathbf{k}_t(n,m) = \hat{\mathbf{x}}\left\{\left[\beta_{x0} + 2\pi\left(\frac{n}{a_1\cos\phi} - \frac{m\sin\phi}{a_2\cos\phi}\right)\right] - j\alpha_x\right\}$$

$$+ \hat{\mathbf{y}}\left[\left(\beta_{y0} + 2\pi\frac{m}{a_2}\right) - j\alpha_y\right] \quad (8)$$

$$k_z(n,m) = \sqrt{k^2 - \mathbf{k}_t(n,m)\cdot\mathbf{k}_t(n,m)} \quad (9)$$

$$E = \max\left(\sqrt{\frac{\pi}{S_U}}, \frac{k}{2H}\right) \quad (10)$$

where $\mathrm{erfc}(\cdot)$ is the complex error function, and the numerical evaluation of $\mathrm{erfc}(\cdot)$ can be found in [11]. E is the splitting parameter, and in (10) H^2 is the maximum exponent permitted [8].

In numerical algorithms, there are cases where we also need to use the gradient of the Green's function. The gradient of the two-dimensional periodic Green's function based on the Ewald method is expressed as follows.

$$\nabla G_p(\mathbf{R}) = \nabla G_{spat}(\mathbf{R}) + \nabla G_{spec}(\mathbf{R}) \quad (11)$$

$$\nabla G_{spat}(\mathbf{R}) = -\frac{1}{8\pi}\sum_{n,m}\mathbf{R}_{nm}e^{-j\boldsymbol{\beta}_0\cdot\boldsymbol{\rho}_{nm}}$$

$$\cdot\sum_{\pm}e^{\pm jkR_{nm}}\left[\begin{array}{c}\frac{\mp jkR_{nm}+1}{R_{nm}^3}\mathrm{erfc}\left(R_{nm}E \pm \frac{jk}{2E}\right) \\ + \frac{2E}{\sqrt{\pi}R_{nm}^2}e^{-\left(R_{nm}E+\frac{jk}{2E}\right)^2}\end{array}\right] \quad (12)$$

$$\nabla G_{spec}(\mathbf{R}) = \hat{\mathbf{x}}\frac{dG_{spec}(R)}{dx} + \hat{\mathbf{y}}\frac{dG_{spec}(R)}{dy} + \hat{\mathbf{z}}\frac{dG_{spec}(R)}{dz} \quad (13)$$

In (13),

$$\frac{dG_{spec}(R)}{dx} = -jk_{tx}(n,m)\frac{1}{4S_U}\sum_{n,m}\frac{e^{-j\mathbf{k}_t(n,m)\cdot\mathbf{R}}}{jk_z(n,m)}$$
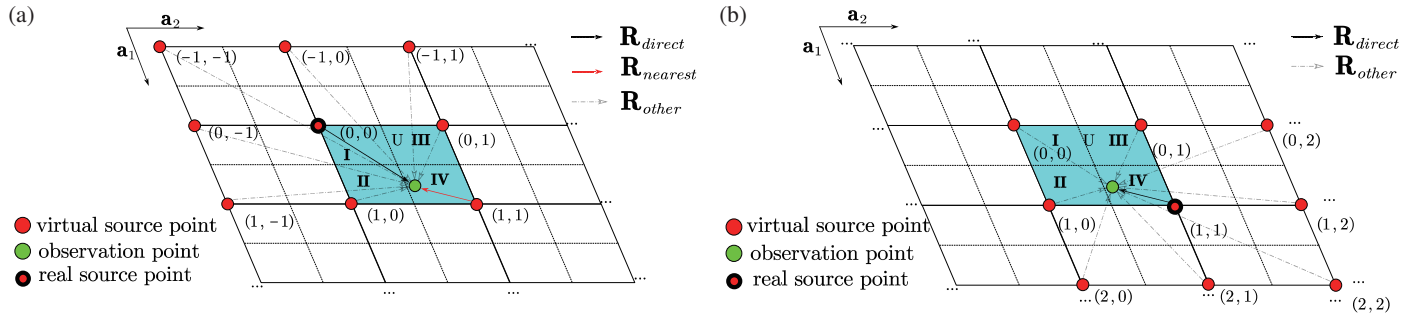
FIGURE 2. Diagram of the interactions between the source points and the observation point of Green's functions (a) G_{p1} and (b) G_{p2}.

$$\cdot \sum_{\pm} e^{\pm j Z k_z(n,m)} \text{erfc} \left(\frac{j k_z(n,m)}{2E} \pm ZE \right) \tag{14a}$$

$$\frac{dG_{spec}(R)}{dy} = -j k_{ty}(n,m) \frac{1}{4S_U} \sum_{n,m} \frac{e^{-j \mathbf{k}_t(n,m) \cdot \mathbf{R}}}{j k_z(n,m)}$$

$$\cdot \sum_{\pm} e^{\pm j Z k_z(n,m)} \text{erfc} \left(\frac{j k_z(n,m)}{2E} \pm ZE \right) \tag{14b}$$

$$\frac{dG_{spec}(R)}{dz} = \frac{1}{4S_U} \sum_{n,m} \frac{e^{-j \mathbf{k}_t(n,m) \cdot \mathbf{R}}}{j k_z(n,m)}$$

$$\cdot \sum_{\pm} e^{\pm j Z k_z(n,m)} \left[\begin{array}{c} \pm j k_z(n,m) \, \text{erfc} \left(\frac{j k_z(n,m)}{2E} \pm ZE \right) \\ \mp \frac{2E}{\sqrt{\pi}} e^{- \left(\frac{j k_z(n,m)}{2E} \pm ZE \right)^2} \end{array} \right] \tag{14c}$$

The Ewald series converge very fast. In most scenarios, series terms with $|n|, |m| < 3$ are sufficient to meet the desired calculation accuracy. In actual calculations of these series, we start by calculating the $(0,0)$th term, and then calculate the (n,m)th terms where $|n| + |m| = 1, 2, 3 \ldots$, until the threshold is met. In our calculations, the threshold is set as $1e-10$.

3. INTERPOLATING STRATEGY

The objective of this section is to efficiently obtain the Green's function of any observation point within the entire space U using an interpolation table. The interpolation strategy consists of two steps: the first step is to construct the interpolation table, and the second step is to retrieve the value of Green's function at a specific observation point through interpolation from the table. Among these steps, constructing the interpolation table is the most time-consuming process.

3.1. Three Properties of Periodic Green's Function

The construction of the new interpolation table requires three properties of the periodic Green's functions. These three properties are listed as follows.

Property 1: translational invariance

This is the fundamental property of Green's functions and their gradients. This property states that when the source point and the observation point in space are translated along the same vector, the Green's function remains unchanged, i.e.,

$$G_p(\mathbf{r}, \mathbf{r}') = G_p(\mathbf{r} + \mathbf{t}, \mathbf{r}' + \mathbf{t}) \tag{15}$$

This property holds true for any arbitrary translation vector $\mathbf{t}$. By utilizing this property, all source points can be translated to a specified position, and then the Green's function at the translated observation point can be studied.

Property 2: periodic phase shift

This is a specific property of the periodic Green's function and its gradient. By using this property, the Green's function within the whole U can be expressed in terms of the Green's function within one-quarter of U. We will now focus on how to represent the periodic Green's function that acts beyond one-quarter of U using the periodic Green's function within one-quarter of U.

Take the situation shown in Figure 2(a) as an example. We divide U into four parts, namely I, II, III, and IV. We now study the periodic Green's function of the source point and the observation point indicated in the figure, denoted as G_{p1}. It is evident that the vector from the real source point to the observation point goes beyond one-quarter of the periodic unit. According to (1), the periodic Green's function includes interactions between an infinite number of source points (including real and virtual source points) and the observation point (Notice that Figure 2(a) only illustrates the vector between the real source point and observation point, as well as the vectors between eight virtual source points within the surrounding units of U and the observation point.). We label the vector from the real source point to the observation point as $\mathbf{R}_{direct}$. Since the observation point falls within IV, the vector from the virtual source point in the $(1,1)$th unit to the observation point is the closest, and we label this vector as $\mathbf{R}_{nearest}$, while other vectors from the virtual source points to the observation point are labeled as $\mathbf{R}_{other}$.

Now let us take a look at the source-to-observation interactions of Green's function G_{p2} shown in Figure 2(b). In Figure 2(b), the observation point remains in the same position as that in Figure 2(a), but the real source point is placed at the location of the source point with $\mathbf{R}_{nearest}$. It is not difficult to see that the periodic Green's functions represented by Figure 2(a) and Figure 2(b) contain exactly the same set of $\mathbf{R}_{nm}$, but due to the different placement of the real source point, these two Green's functions differ only by a phase factor. Specifically, for Figure 2(a) and Figure 2(b), this phase factor is $e^{j \boldsymbol{\beta}_0 \cdot \boldsymbol{\rho}_{nm}}$, namely

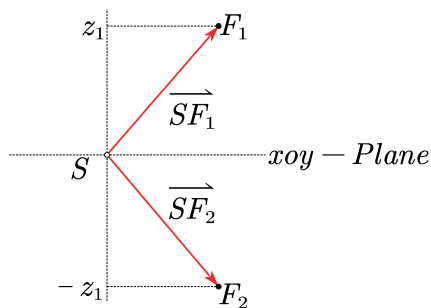$$G_{p1} = e^{j \boldsymbol{\beta}_0 \cdot \boldsymbol{\rho}_{nm}} G_{p2} \tag{16}$$

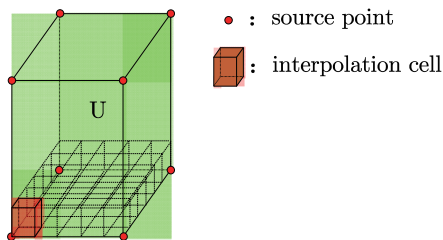FIGURE 3. Diagram of mirror points.

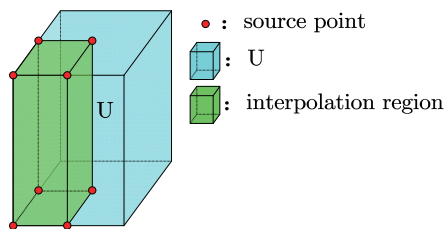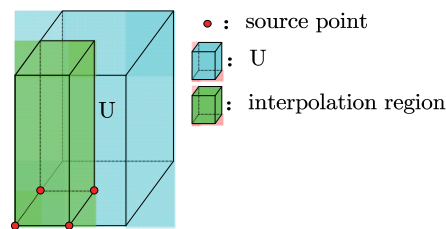FIGURE 4. Region for Interpolation Table 1.   FIGURE 5. Region for Interpolation Table 2.   FIGURE 6. Region for Interpolation Table 3.

Similar conclusion can be made for the situations where the observation point is put in II or III. In a word, by utilizing the periodic-phase-shift property, the periodic Green's function that acts beyond one-quarter of the unit can be expressed in terms of the periodic Green's function that acts within one-quarter of the unit.

Property 3: vertical symmetry

Consider the scenario depicted in Figure 3. In Figure 3, the observation points F_1 and F_2 are mirror symmetric about the *xoy* plane, while the source point S is located within the *xoy* plane. For the periodic Green's function, the phase term constrained by Floquet's theorem only affects the transverse factor. Therefore, in Figure 3, the periodic Green's functions corresponding to F_1 and F_2 are the same, but the z-components of the gradient of the periodic Green's functions corresponding to F_1 and F_2 are opposite to each other.

3.2. Construction of the Minimal Interpolation Table

If we consider only the first property of the periodic Green's function, then region of the interpolation table for the periodic Green's function is as shown in Figure 4. Interpolation table with this interpolation region is denoted as Interpolation Table 1.

In Figure 4, the green region represents the region for constructing the interpolation table, which is also the whole U. We divide U into n, m, and p segments along the $\mathbf{a}_1$, $\mathbf{a}_2$, and $\mathbf{z}$ directions, respectively, resulting in a total of nmp small cells, with each small cell called an interpolation cell. Considering that the Green's function needs to encompass all directions in three-dimensional space, the eight vertices of U are set as real source points. The eight vertices of each interpolation cell are the observation points to be recorded. As a result, Interpolation Table 1 requires precomputing $(m + 1)(n + 1)(p + 1) \cdot 8$

values of the periodic Green's function. Conventionally, Interpolation Table 1 is the most widely used.

Next, if we also consider the second property of the periodic Green's function, then the interpolation region for the interpolation table would be as shown in Figure 5. Interpolation table with this interpolation region is denoted as Interpolation Table 2. If we use interpolation cells of the same size as Interpolation Table 1, then Interpolation Table 2 would require precomputing a total of $[(n + 1)/2][(m + 1)/2](p + 1) \cdot 8$ values of the periodic Green's function.

Finally, when we consider all of the three properties, we obtain the interpolation region shown in Figure 6. The interpolation table with this interpolation region is denoted by Interpolation Table 3. Compared to Interpolation Table 2, Interpolation Table 3 has four fewer source points. If we use interpolation cells of the same size as Interpolation Table 1, Interpolation Table 3 would require precomputing a total number of $[(n + 1)/2][(m + 1)/2](p + 1) \cdot 4$ values of the periodic Green's function. It can be seen that, with the same interpolation cell size, Interpolation Table 3 is one-eighth the size of Interpolation Table 1 (which is the most commonly used one). Using (2), (3), and (4), the calculation time for each periodic Green's function value is similar, thus, it is evident that the construction time for Interpolation Table 3 is approximately one-eighth of the construction time for Interpolation Table 1. We refer to Interpolation Table 3 as the minimal interpolation table.

3.3. Extraction of Singular Terms

To construct an interpolation table, using nonuniform cells [8] near the source points to handle the Green's function's rapid variation is cumbersome. In free and periodic space, after removing the singular terms, the remaining part of Green's func-

tion exhibits good smoothness. Thus, we construct the table with this "smooth" Green's function for linear interpolation. Singular terms are reintroduced later for the final results.

For nearly square periodic units, extract the singular term from the $(0, 0)$th unit suffices. In this case, the smooth Green's function (G_{sp}) and its gradient (∇G_{sp}) can be represented as follows

$$G_{sp}(R) = G_p(R) - \frac{e^{-j\boldsymbol{\beta}_0 \cdot \boldsymbol{\rho}_{00}}}{4\pi R_{00}} \tag{17}$$

$$\nabla G_{sp}(\mathbf{R}) = \nabla G_p(\mathbf{R}) + \left(\frac{k^2 \mathbf{R}_{00}}{8\pi R_{00}} + \frac{\mathbf{R}_{00}}{4\pi R_{00}^3}\right) e^{-j\boldsymbol{\beta}_0 \cdot \boldsymbol{\rho}_{00}} \tag{18}$$

However, when we need to deal with units that have extremely skewed transverse sections, the singular terms corresponding to the surrounding units of the $(0, 0)$th unit also need to be extracted. In this case, the smooth Green's function and its gradient should be expressed as:

$$G_{sp}(R) = G_p(R) - \sum_{|n,m|<2} \frac{e^{-j\boldsymbol{\beta}_0 \cdot \boldsymbol{\rho}_{nm}}}{4\pi R_{nm}} \tag{19}$$

$$\nabla G_{sp}(\mathbf{R}) = \nabla G_p(\mathbf{R})$$
$$+ \sum_{|n,m|<2} \left(\frac{k^2 \mathbf{R}_{nm}}{8\pi R_{nm}} + \frac{\mathbf{R}_{nm}}{4\pi R_{nm}^3}\right) e^{-j\boldsymbol{\beta}_0 \cdot \boldsymbol{\rho}_{nm}} \tag{20}$$

It means that a total of nine singular terms need to be removed.

Finally, when constructing the interpolation table, there is also the situation where the source point coincides with the field point. Numerically, this can be handled by applying a small offset. In practice, we offset the observation point outward along the $\mathbf{a}_1$, $\mathbf{a}_2$, and $\mathbf{z}$ directions by $1e - 8\,\text{m}$. This approach can achieve satisfactory accuracy in common microwave frequency bands.

3.4. Linear Interpolation

With the help of three properties of periodic Green's functions, we can always locate the observation point of any Green's function inside a unit within the minimal interpolation table. Within the interpolation cell, using the values of the smooth Green's function at the eight vertices of the interpolation cell, we can obtain the value of the smooth Green's function at the observation point through linear interpolation. Linear interpolation can be performed as follows.

As shown in Figure 7, P_1 to P_8 are the eight vertices of the interpolation cell; P_p is the observation point within that cell; and P_{p1} and P_{p2} are the vertical projection points of P_p on the lower and upper faces of the interpolation cell, respectively. During interpolation, the first step is to use two-dimensional linear interpolation based on the information of points P_1 to P_4 and P_5 to P_8 to obtain the values of the smooth Green's function at P_{p1} and P_{p2}. Then, based on the information of P_{p1} and P_{p2}, one-dimensional linear interpolation is used to finally obtain the value of the smooth Green's function at P_p.
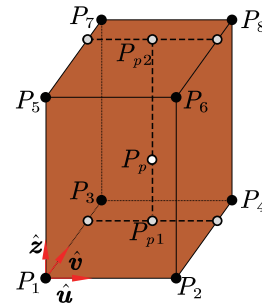

FIGURE 7. Linear interpolation in an interpolation cell.

3.5. Process of the Interpolation Scheme

After constructing the interpolation table using the smooth Green's function within the interpolation region shown in Figure 6, the process of obtaining the Green's function and its gradient of given source point P_s and observation point P_f using the interpolation algorithm can be summarized as follows:

Step 1: Obtain the vector P_{sf} from P_s to P_f by using coordinates of P_s and P_f.

Step 2: Translate P_{sf} so that P_s is located at one of the vertices of U, while ensuring that P_f is inside U.

Step 3: Utilize Property 2 to map P_{sf} onto the interpolation region shown in Figure 5, denoting the corresponding vector as P'_{sf}. Notice that the source point of P'_{sf} lies at one of the vertices of the interpolation region. G_{sp} and ∇G_{sp} of P'_{sf} are the same as those of P_{sf}.

Step 4: If the vertical coordinate of P'_{sf} is greater than or equal to 0, then G_{sp} and ∇G_{sp} of P'_{sf} can be directly obtained through linear interpolation within the interpolation table. If the vertical coordinate of P'_{sf} is less than 0, first negate the vertical coordinate of P'_{sf} to obtain P''_{sf}, and then use linear interpolation within the interpolation table to obtain G_{sp} and ∇G_{sp} of P''_{sf}. G_{sp} of P''_{sf} is the same as that of P'_{sf}, while the z-component of ∇G_{sp} of P''_{sf} needs to be negated to obtain the correct ∇G_{sp} of P'_{sf}.

Step 5: Add back the singular terms corresponding to G_{sp} and ∇G_{sp} to obtain the final values of the periodic Green's function and its gradient.

4. NUMERICAL EXAMPLES

In this section, two numerical examples are given to compare the results obtained by the interpolation method described in the text with the series results obtained by the Ewald method.

The first example considers a periodic unit with a square transverse section, as shown in Figure 8. The transverse periodic vectors of the unit are $\mathbf{a}_1 = (15, 0)$ and $\mathbf{a}_2 = (0, 15)$. The source point for the periodic Green's function is placed at one vertex of the unit U, and the observation points are located along a sampling line. The sampling line is parallel to the *xoy* plane and is positioned 0.15 mm above the source point. There are 1000 sampling points on the sampling line. The working frequency is set at 10 GHz, and the angles of incident wave are $\theta^{\text{inc}} = 45°$ and $\phi^{\text{inc}} = 30°$, respectively. The edge length of the interpolation cell is chosen as $1/30\lambda$. In this example, the
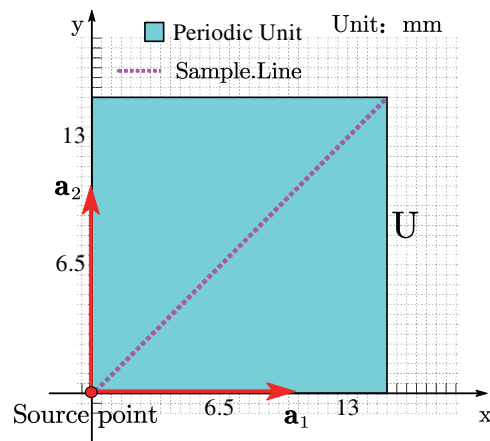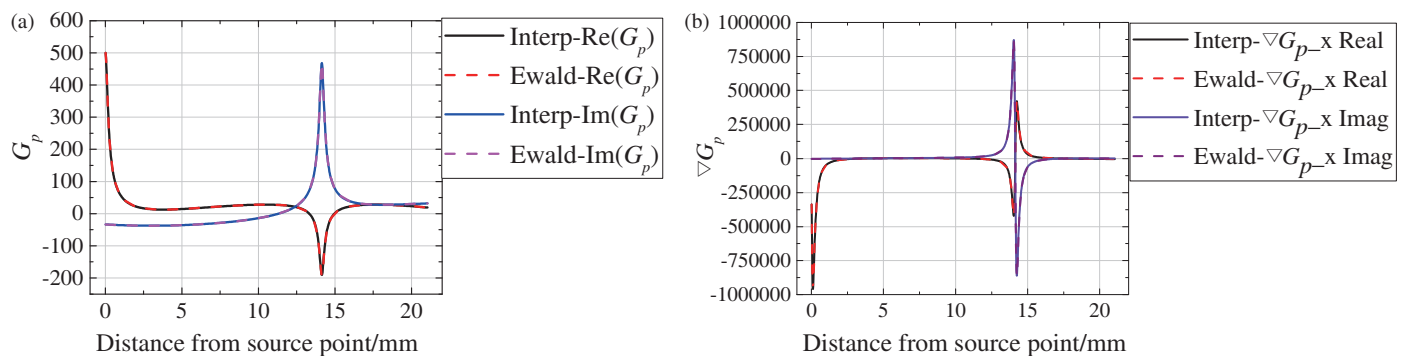
FIGURE 8. Square periodic unit.

FIGURE 9. Values of (a) G_p and (b) ∇G_p of different methods.
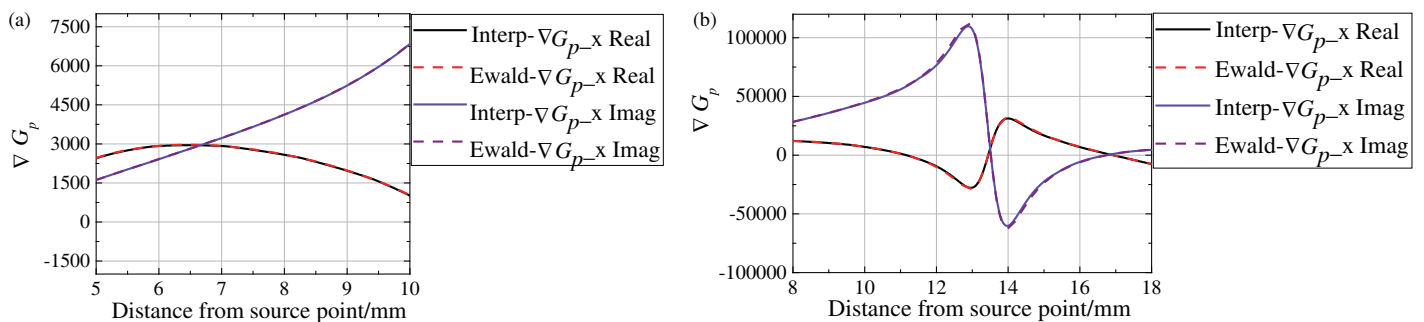

FIGURE 10. Enlarged views 0f the local details of Figure 9(b). (a) Detail 1 and (b) detail 2.

smooth Green's function only excludes the singular terms of the $(0, 0)$th unit.

Figure 9(a) presents the results of real and imaginary parts of the Green's function, and Figure 9(b) shows the results of the real and imaginary parts of the x component of the gradient of the Green's function. In Figure 9, the dashed lines represent the results directly obtained by the Ewald series method, while the solid lines represent the results obtained by the interpolation method of Subsection 3.5. Figure 10 gives enlarged views of the local details of Figure 9(b). It can be observed that the interpolation results align well with the actual values of the Green's function and its gradient, indicating that in this case, it is suf-

ficient to just exclude the singular terms of the $(0, 0)$th unit to get satisfactory accuracy.

The second example considers a periodic unit with an extremely skewed parallelogram transverse section, as shown in Figure 11. The transverse periodic vectors of the unit are $\mathbf{a}_1 = (10, 9)$ and $\mathbf{a}_1 = (9, 10)$. The source point for the periodic Green's function is placed at one vertex of the unit U, and the observation points are located along a sampling line. The sampling line is parallel to the xoy plane and is positioned $0.15\,\mathrm{mm}$ above the source point. There are 1000 sampling points on the sampling line. The working frequency is set at $10\,\mathrm{GHz}$, and the angles of incident field are $\theta^{\mathrm{inc}} = 45°$ and $\phi^{\mathrm{inc}} = 30°$, respectively. The side length of the interpolation cell is chosen
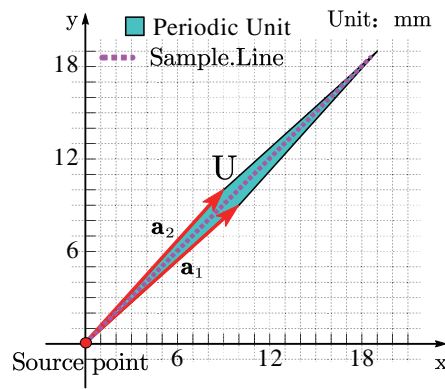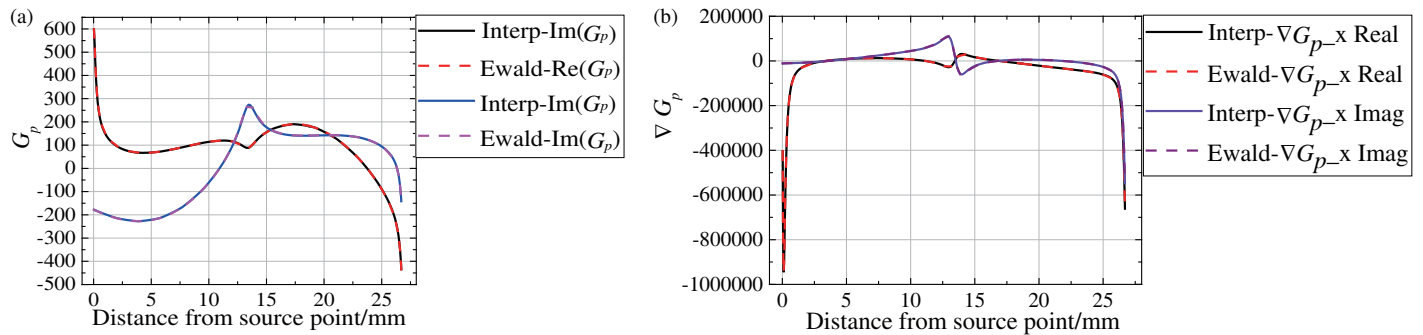
FIGURE 11. Skewed parallelogram unit.

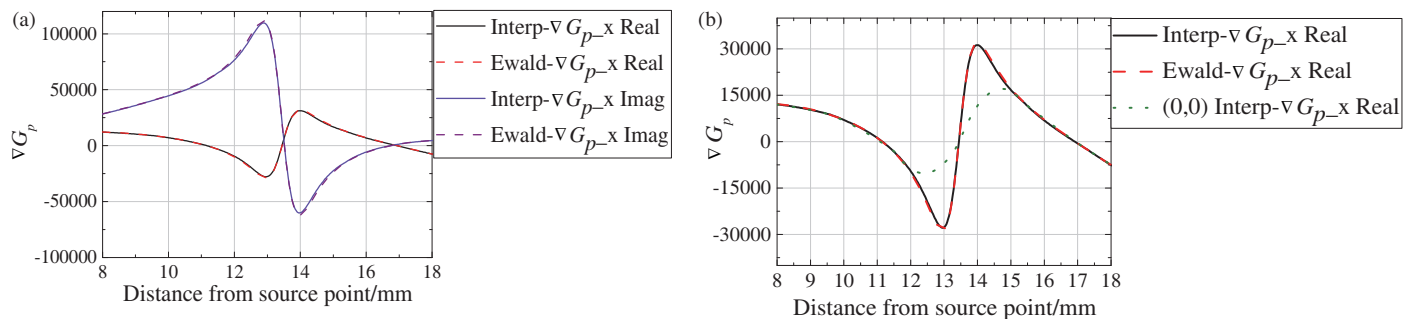**FIGURE 12**. Values of (a) G_p and (b) ∇G_p of different methods.

FIGURE 13. (a) Enlarged views of the local details of Figure 12(b). (b) Interpolation results with different ∇G_{sp}.

as $1/30\lambda$. In this example, all singular terms are excluded from the smoothed Green's function.

Figure 12(a) presents the results of the real and imaginary parts of the Green's function, and Figure 12(b) shows the results of the real and imaginary parts of the x component of the gradient of the Green's function. In Figure 12, the dashed line represents the results directly obtained by the Ewald series method, while the solid line represents the results obtained by the interpolation method of Subsection 3.1. Figure 13(a) is an enlarged view of the local details of Figure 12(b). It can be observed that the interpolation results align well with the actual values of the Green's function and its gradient.

Furthermore, it should be noted that for the scenario shown in Figure 11, if the smooth Green's function in the interpolation table only excludes the singular terms of the $(0,0)$th unit,

the obtained results are not satisfactory. Figure 13(b) compares the interpolation results with different ∇G_{sp}. The dotted lines represent the interpolation results using the ∇G_{sp} that excludes only the singular terms of the $(0,0)$th unit. It can be seen that excluding only the singular terms of the $(0,0)$th unit is not sufficiently accurate in this case. To address general scenarios, it is necessary to exclude all singular terms when constructing the interpolation table for the smooth Green's function and its gradient.

5. CONCLUSION

This paper first proposes a construction strategy for a minimal interpolation table of 2D periodic Green's functions, which is one-eighth the size of a traditional interpolation table. The min-

imal interpolation table fully utilizes three properties of the periodic Green's function, namely, translational invariance, periodic phase shift, and vertical symmetry. In contrast, a traditional interpolation table only utilizes the translational invariance of the Green's function. The construction of the interpolation table employs smooth Green's functions, which require the exclusion of all singular terms to meet the accuracy requirements of general scenarios. After obtaining the desired smooth Green's functions through linear interpolation in the interpolation table, the singular terms are added back to obtain the final values of the Green's functions. Numerical results demonstrate the accuracy and effectiveness of the proposed interpolation method, making it suitable for electromagnetic field calculations and analysis of periodic structures when being combined with numerical methods.

REFERENCES

[1] Munk, B. A., *Frequency Selective Surfaces: Theory and Design*, John Wiley & Sons, 2005.

[2] Amitay, N., V. Galindo, and C. P. Wu, "Theory and analysis of phased array antennas," *Theory and Analysis of Phased Array Antennas*, 1972.

[3] Holloway, C. L., E. F. Kuester, J. A. Gordon, J. O'Hara, J. Booth, and D. R. Smith, "An overview of the theory and applications of metasurfaces: The two-dimensional equivalents of metamaterials," *IEEE Antennas and Propagation Magazine*, Vol. 54, No. 2, 10–35, Apr. 2012.

[4] Valerio, G., P. Baccarelli, P. Burghignoli, and A. Galli, "Comparative analysis of acceleration techniques for 2-D and 3-D Green's functions in periodic structures along one and two directions," *IEEE Transactions on Antennas and Propagation*, Vol. 55, No. 6, 1630–1643, Jun. 2007.

[5] Jordan, K. E., G. R. Richter, and P. Sheng, "An efficient numerical evaluation of the Green's function for the Helmholtz operator on periodic structures," *Journal of Computational Physics*, Vol. 63, No. 1, 222–235, 1986.

[6] Singh, S. and R. Singh, "On the use of shank's transform to accelerate the summation of slowly converging series," *IEEE Transactions on Microwave Theory and Techniques*, Vol. 39, No. 3, 608–610, Mar. 1991.

[7] Jorgenson, R. E. and R. Mittra, "Efficient calculation of the free-space periodic Green's function," *IEEE Transactions on Antennas and Propagation*, Vol. 38, No. 5, 633–642, May 1990.

[8] Stevanovic, I., P. Crespo-Valero, K. Blagovic, F. Bongard, and J. R. Mosig, "Integral-equation analysis of 3-D metallic objects arranged in 2-D lattices using the Ewald transformation," *IEEE Transactions on Microwave Theory and Techniques*, Vol. 54, No. 10, 3688–3697, Oct. 2006.

[9] Dardenne, X. and C. Craeye, "Method of moments simulation of infinitely periodic structures combining metal with connected dielectric objects," *IEEE Transactions on Antennas and Propagation*, Vol. 56, No. 8, 2372–2380, Aug. 2008.

[10] Hu, F.-G. and J. Song, "Integral-equation analysis of scattering from doubly periodic array of 3-D conducting objects," *IEEE Transactions on Antennas and Propagation*, Vol. 59, No. 12, 4569–4578, Dec. 2011.

[11] Poppe, G. P. M. and C. M. J. Wijers, "More efficient computation of the complex error function," *ACM Transactions on Mathematical Software*, Vol. 16, No. 1, 38–46, Mar. 1990.